ministered in vivo, somatotropin induces amounts of O_2^- similar to those produced by IFN-γ at a concentration that is optimal for macrophage activation (*18*). Thus, somatotropin shares at least one biologic activity with IFN-γ, priming macrophages to produce augmented amounts of O_2^-. It will be important to learn whether other macrophage-activating properties of IFN-γ are also shared by somatotropin.

These data expand earlier results that have shown that somatotropin is involved in the regulation of immune events in vivo (*10–14*). Macrophages are central to the induction and expression of many immune responses, so perhaps a fundamental mechanism of action of somatotropin is at the level of macrophages. Since we used animals that had their pituitary source of somatotropin removed, these results may be particularly important for growth hormone–deficient children who receive exogenous recombinant somatotropin to stimulate growth. Although excessive amounts of reactive oxygen metabolites can damage host tissues and can kill intracellular bacteria (*20*), we believe that this discovery of macrophages as one target for the action of somatotropin is important for understanding reciprocal relationships between the immune and endocrine systems (*21*).

REFERENCES AND NOTES

1. G. B. Mackaness, *J. Exp. Med.* **129**, 973 (1969); D. O. Adams and T. A. Hamilton, *Annu. Rev. Immunol.* **2**, 283 (1984).
2. B. M. Babior, *N. Engl. J. Med.* **298**, 659 (1978); R. B. Johnston, Jr., *Lymphokines* **3**, 33 (1981); C. F. Nathan, M. I. Karnovsky, J. R. David, *J. Exp. Med.* **133**, 1356 (1971).
3. C. F. Nathan, H. W. Murray, M. E. Wiebe, B. Y. Rubin, *J. Exp. Med.* **158**, 670 (1983); H. W. Murray, G. Spitalny, C. F. Nathan, *J. Immunol.* **134**, 1619 (1985); C. M. Black, J. R. Catterall, J. S. Remington, *J. Immunol.* **138**, 491 (1987).
4. C. F. Nathan *et al.*, *J. Exp. Med.* **160**, 600 (1984).
5. H. W. Murray *et al.*, *N. Engl. J. Med.* **310**, 883 (1984); H. C. Lane *et al.*, *ibid.* **313**, 79 (1985); H. W. Murray *et al.*, *ibid.*, p. 1504; H. W. Murray *et al.*, *J. Immunol.* **138**, 2457 (1987).
6. N. Nogueira *et al.*, *J. Exp. Med.* **158**, 2165 (1983); C. F. Nathan *et al.*, *N. Engl. J. Med.* **315**, 6 (1986).
7. E. M. Carvalho, R. Badaró, S. G. Reed, T. C. Jones, W. D. Johnson, Jr., *J. Clin. Invest.* **76**, 2066 (1985); C. F. Nathan *et al.*, *J. Immunol.* **138**, 2290 (1987).
8. M. S. Cohen, D. E. Mesler, R. G. Snipes, T. K. Gray, *J. Immunol.* **136**, 1049 (1986); E. J. Wing, N. M. Ampel, A. Waheed, R. K. Shadduck, *ibid.* **135**, 2052 (1985); R. D. Schreiber, L. J. Hicks, A. Celada, N. A. Buchmeier, P. W. Gray, *ibid.* **134**, 1609 (1985); C. A. Nacy, A. H. Fortier, M. S. Meltzer, N. A. Buchmeier, R. D. Schreiber, *ibid.* **135**, 3505 (1985); P. H. Krammer, C. F. Kubelka, W. Falk, A. Ruppel, *ibid.*, p. 3258; H. P. Hartung and K. V. Toyka, *Eur. J. Pharmacol.* **89**, 301 (1983).
9. P. C. Hiestand *et al.*, *Proc. Natl. Acad. Sci. U.S.A.* **83**, 2599 (1986).
10. K. W. Kelley *et al.*, *ibid.*, p. 5663; D. R. Davila *et al.*, *J. Neurosci. Res.* **18**, 108 (1987).
11. C. Snow, T. L. Feldbush, J. A. Oaks, *J. Immunol.* **126**, 161 (1981).
12. W. Kiess, H. Doerr, E. Eisl, O. Butenandt, B. H. Belohradsky, *N. Engl. J. Med.* **314**, 321 (1986); O. B. Saxena, R. K. Saxena, W. H. Adler, *Int. Arch. Allergy Appl. Immunol.* **67**, 169 (1982).
13. E. Nagy, H. G. Friesen, A. H. Sehan, I. Berczi, *Endocrinology* **116**, 1117 (1985); W. Pierpaoli, C. Baroni, N. Fabris, E. Sorkin, *Immunology* **16**, 217 (1969); N. Fabris, W. Pierpaoli, E. Sorkin, *Clin. Exp. Immunol.* **9**, 227 (1971).
14. B. L. Goff, J. A. Roth, L. H. Arp, G. S. Incefy, *Clin. Exp. Immunol.* **68**, 580 (1987); N. Fabris, E. Mocchegiani, P. Paolucci, A. Balsamo, E. Cacciari, *Clin. Exp. Immunol.*, in press.
15. E. R. Unanue and P. M. Allen, *Science* **236**, 551 (1987); S. E. Loveless and G. H. Heppner, *J. Immunol.* **131**, 2074 (1983); K. H. Mahoney, A. M. Fulton, G. H. Heppner, *ibid.*, p. 2079.
16. M. J. Pabst and R. B. Johnston, Jr., *J. Exp. Med.* **151**, 101 (1980).
17. D. N. Marple and E. D. Aberle, *J. Anim. Sci.* **34**, 261 (1972).
18. C. K. Edwards III *et al.*, *J. Immunol.* **136**, 1820 (1986).
19. A. M. Badger, *J. Leukocyte Biol.* **40**, 725 (1986); S. J. Leibovich and R. Ross, *Am. J. Pathol.* **78**, 71 (1975).
20. B. Halliwell, *FASEB* **1**, 358 (1987).
21. J. E. Blalock, *Lymphokines* **9**, 1 (1984); K. W. Kelley, *J. Anim. Sci.*, in press.
22. R. L. McGuire and L. A. Babiuk, *J. Reticul. Soc.* **31**, 251 (1982); B. Charley, *Ann. Rech. Vet.* **13**, 1 (1982); H. Bielefeldt Ohmann and L. A. Babiuk, *J. Leukocyte Biol.* **39**, 167 (1986); F. Y. El-Awar and E. C. Hahn, *Am. J. Vet. Res.* **48**, 481 (1987); D. O. Slauson, J. C. Lay, W. L. Castleman, N. R. Neilsen, *ibid.* **41**, 412 (1987).
23. R. B. Johnston, C. A. Godzik, Z. A. Cohn, *J. Exp. Med.* **148**, 115 (1978); P. R. Gangadharam and C. K. Edwards III, *Am. Rev. Respir. Dis.* **130**, 834 (1984).
24. *SAS User's Guide: Statistics* (SAS Institute, Cary, NC, 1985).
25. C. Haslett, L. A. Guthrie, M. M. Kopaniak, R. B. Johnston, Jr., P. M. Henson, *Am. J. Pathol.* **119**, 101 (1985); R. A. Musson, *ibid.* **111**, 331 (1983).

26. We thank S. Raiti for supplying native, pituitary-derived rat somatotropin; A. F. Parlow for supplying native, pituitary-derived porcine somatotropin; IMC Pitman-Moore, Inc., for furnishing recombinant porcine somatotropin; R. Dantzer, L. Schook, H. Lewin, J. Simon, and D. Kranz for helpful suggestions with this manuscript, and L. Martin, D. Tully, S. Brief, and R. Franklin for technical assistance. This research was supported in part by NIH grant AG06246-01, U.S. Department of Agriculture grant 86-CRCR-1-2003, and IMC Pitman-Moore grant K-0503 and by Illinois Agriculture Experiment Station project 20-0386 (to K.W.K.).

14 September 1987; accepted 31 December 1987

Subset-Specific Expression of Potassium Channels in Developing Murine T Lymphocytes

RICHARD S. LEWIS AND MICHAEL D. CAHALAN

Ion channels were studied in four major subsets of developing murine thymocytes by using patch-clamp recording and cell-surface staining techniques. The expression of three types of voltage-gated potassium channels in thymocytes varies consistently with the cell's developmental state and functional class as defined by cell-surface markers. One class of potassium channel (type *n*) predominates in immature thymocyte subsets as well as in mature-phenotype $CD4^+CD8^-$ thymocytes (precursors to helper T lymphocytes), and the average surface density of this channel type correlates with the extent of cell proliferation. Two additional types of potassium channels (types *n'* and *l*) are found in the mature $CD4^-CD8^+$ thymocyte subset that contains precursors to cytotoxic and suppressor T cells. The subset-specific expression of type *n'* and *l* potassium channels suggests their use as additional cell-surface markers with which to identify precursors to the cytotoxic suppressor T cell lineage.

THE MOST PREVALENT VOLTAGE-GATED channels in mature T lymphocytes are potassium channels, similar in several respects to delayed rectifier channels of nerve and muscle (*1–5*). At least two distinct types of voltage-gated K^+ channels have been observed in T lymphocytes from mice (*5, 6*), but their developmental origins and distribution among the several functional classes of T cells have not been determined. To investigate this question, we have applied patch-clamp recording techniques (*7*) to subsets of developing T cells in the murine thymus. Thymocyte subsets were identified by staining with fluorescently labeled monoclonal antibodies to CD4 (L3T4) and CD8 (Lyt-2) membrane glycoproteins or with fluorescently labeled peanut agglutinin (PNA). Functionally immature thymocytes are generally $CD4^-CD8^-$ (double-negative) or $CD4^+CD8^+$ (double-positive; also PNA^+), whereas the phenotypes of the remaining thymocytes are the same as those of mature T cells; that is, $CD4^+CD8^-$ or $CD4^-CD8^+$ (*8–10*). After phenotypic identification by epifluorescence microscopy (*11*) (see cover), each cell was voltage-clamped in the whole-cell or excised-patch recording mode (*7*) to characterize the channels present in its membrane.

In whole-cell recordings from over 200 thymocytes, we observed three types of voltage-dependent K^+ channels, termed *n*, *n'*, and *l*. A set of biophysical and pharmacological properties provides a "fingerprint" for identifying each of the three classes of K^+

Department of Physiology and Biophysics, California College of Medicine, University of California, Irvine, CA 92717.

channels. Type *n* and *l* K^+ channels in peripheral murine T cells have been described (*5, 6*); *n'* channels, not previously characterized, resemble *n* channels in several respects. Most notably, both *n* and *n'*, but not *l* channels, are blocked completely by 5 n*M* charybdotoxin (CTX), a peptide neurotoxin isolated from *Leiurus quinquestriatus* scorpion venom (*12*). We named the third channel type *n'* because the high affinity block by CTX may indicate structural homology between this channel and *n* channels (*13*). Additional properties that distinguish the three channel classes include the voltage dependence of activation, the degree to which channels are inactivated during repetitive depolarizations (Fig. 1A), the channel closing rate (Fig. 1B), and the sensitivity to blockade by tetraethylammonium ion (TEA) (Fig. 1C). Consistent with results from mature peripheral T cells (*1–3, 5*), type *n* K^+ channels in thymocytes open at potentials more positive than −40 mV, are cumulatively inactivated during repetitive depolarizations, close relatively slowly at subactivating voltages, and are half-blocked by 10 m*M* TEA. Type *l* channels in thymocytes, like their counterparts in mature T cells (*5*), open only at potentials above −10 mV, display very little cumulative inactivation, close rapidly, and are highly sensitive to TEA blockade [half-blocking dose ($K_{1/2}$), 0.1 m*M*)]. Although type *n'* channels resemble *n* channels in their voltage dependence of activation, closing kinetics, and sensitivity to CTX, they display little or no cumulative inactivation and are less sensitive to TEA block ($K_{1/2}$, 0.1 m*M*). On the basis of their voltage dependence of activation, cumulative inactivation, and TEA sensitivity, we have identified single K^+ channels in excised membrane patches that correspond to the

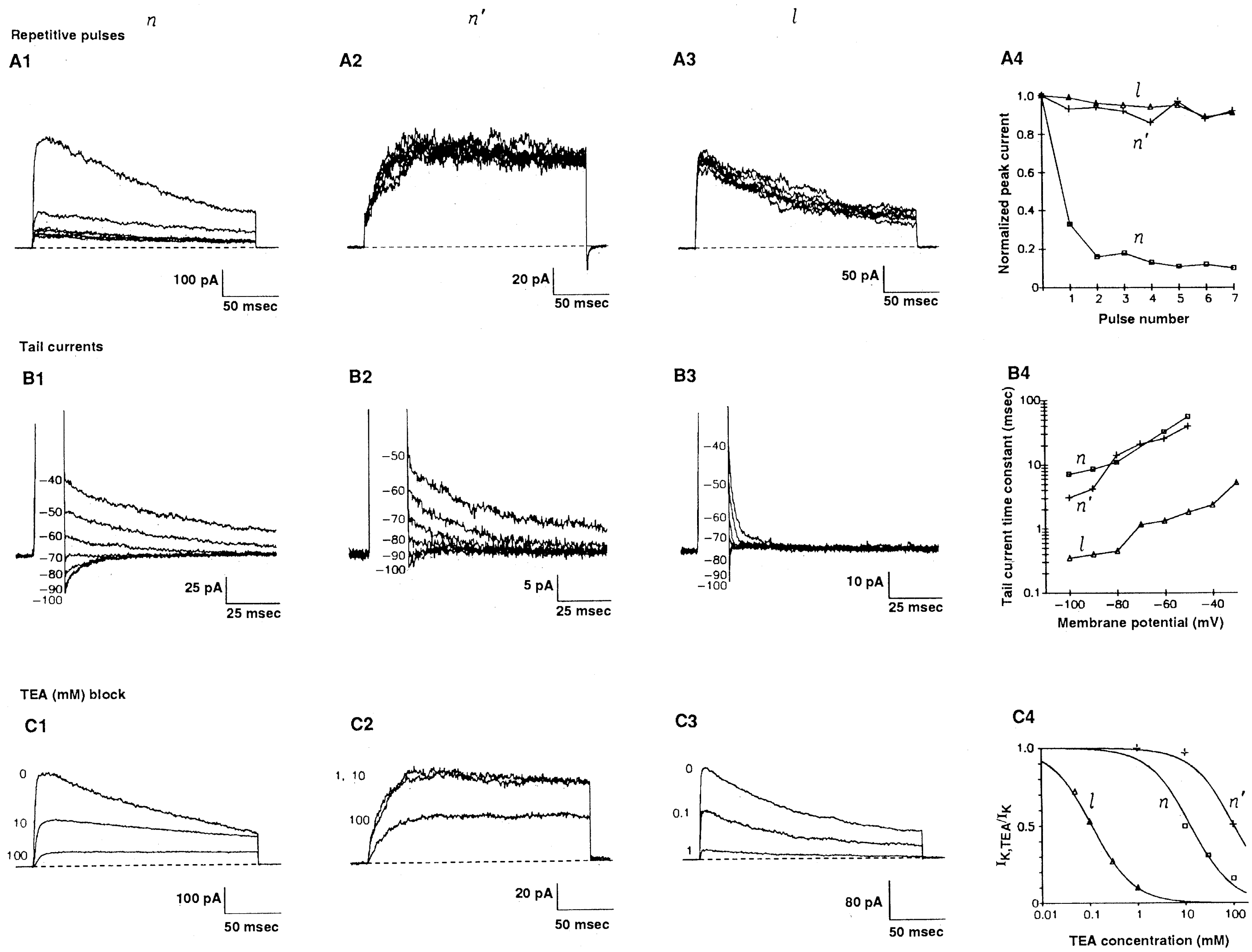

Fig. 1. Characterization of three types of thymocyte K^+ currents. In (A) to (C), columns 1 to 3 represent type *n, n'*, and *l* K^+ currents, respectively, and column 4 summarizes the results. Data were obtained from a PNA^+ cell (column 1) and two $CD4^-CD8^+$ cells (columns 2 and 3). Type *n'* currents were recorded in the presence of 1 m*M* TEA to block any contribution from type *l* channels. (**A**) Cumulative inactivation of potassium current (I_K) during repetitive depolarizations. Voltage stimuli (200-msec pulses from −80 to +30 mV) were delivered at a rate of one per second from a holding potential of −80 mV. Seven responses are superimposed. Peak K^+ current during each pulse is plotted in (A4). (**B**) Voltage dependence of K^+-channel closing rates. Ten- to 20-msec activating pulses from the holding potential (−80 mV) to +30 mV (currents not shown) were followed by pulses of −100 to −40 mV. Exponential curves were fitted to the decay of tail currents at the latter voltages, and the decay time constants are plotted on a log scale against membrane potential in (B4). (**C**) K^+-channel blockade by TEA. K^+ currents were elicited by pulses from −80 to +30 mV in the presence of 0.1 m*M* to 100 m*M* TEA. In (C1), TEA slows the apparent inactivation rate of the K^+ current, not by unmasking a TEA-resistant current component, but through a direct effect on the kinetics of type *n* channels (*26*). The fraction of peak current remaining is plotted against TEA concentration on a log scale. Binding curves (1:1) have been fitted to the data points by eye, corresponding to dissociation constants of 0.1 m*M* (type *l*), 12 m*M* (type *n*), and 100 m*M* (type *n'*). All experiments were conducted at 20° to 24°C by standard recording methods (*7*). Voltage-clamp data were filtered at 2 kHz with an eight-pole Bessel filter and were corrected for linear capacitive and leakage currents. Cells were bathed with Ringer solution: 160 m*M* NaCl, 4.5 m*M* KCl, 2 m*M* $MgCl_2$, 1 m*M* $CaCl_2$, and 5 m*M* Na-Hepes (*p*H 7.4). Pipette (internal) solution contained 134 m*M* KF, 11 m*M* K_2-EGTA, 1.1 m*M* $CaCl_2$, 2 m*M* $MgCl_2$, and 10 m*M* K-Hepes (*p*H 7.2), with less than 2 n*M* free Ca^{2+} (*1*).

three classes of whole-cell currents. The K^+ channels differ in their unitary conductance; values are 18 pS for type *n*, 17 pS for type *n*′, and 27 pS for type *l* channels (Fig. 2).

Both the number and types of K^+ channels present were closely linked to the surface phenotype of each thymocyte subset (Fig. 3). Channel density was estimated from measurements of the maximum K^+ conductance (g_K) and the membrane capacitance of individual cells, quantities proportional to the number of channels and the membrane area, respectively. The types of channels expressed in each cell were identified by the properties described above. Of the four thymocyte subsets we examined, immature thymocytes (that is, double-negative and double-positive cells) displayed a comparatively high surface density of type *n* K^+ channels (Fig. 3A). In the double-negatives, which include the most primitive cells in the thymus (*8–10*), *n* channels were expressed at 1.90 ± 0.41 nS/pF (mean ± SEM, $n = 18$). Assuming a specific membrane capacitance of 1 $\mu F/cm^2$ and a unitary channel conductance of 18 pS, this corresponds to a surface density of ~1 *n* channel per square micrometer of membrane area, or ~100 *n* channels per cell. K^+-channel density was highest in the double-positives. Large cells of this class probably represent cortical blasts, whereas small cells are presumably the blasts' offspring, commonly referred to as small cortical thymocytes (*8–10*). Overall, the mean K^+-channel density of double-positives was 4.77 ± 0.63 nS/pF ($n = 35$), equivalent to ~3 *n* channels per square micrometer of membrane area, or ~300 *n* channels per cell. In our sampling of immature thymocytes we found no definitive evidence for either type *n*′ or *l* channels, suggesting that if these channel types are expressed, they occur either in a small proportion of immature cells, or at a level too low to be detected by our methods (*14*).

In thymocytes with mature phenotypes, the types of K^+ channels expressed were highly correlated with cell-surface phenotype, and hence with immunological function. $CD4^+CD8^-$ thymocytes, primarily precursors to helper T cells that recognize class II antigens of the major histocompatibility complex (MHC) (*15, 16*), displayed type *n* channels at densities one-tenth to one-fifth those of either of the immature thymocyte populations (Fig. 3B). Excluding the few cells in this class with unusually high numbers of channels ($g_K > 3$ nS), the average normalized conductance was 0.40 ± 0.07 nS/pF ($n = 20$), corresponding to ~0.2 *n* channels per square micrometer of membrane area, or ~20 *n* channels per cell. In $CD4^-CD8^+$ thymocytes, principally precursors of cytotoxic or suppressor T cells recognizing MHC class I antigens (*16, 17*), the average normalized conductance was 1.70 ± 0.22 nS/pF ($n = 59$). Unlike the immature and $CD4^+CD8^-$ thymocyte populations, channel expression in the $CD4^-CD8^+$ cells was heterogeneous. In only 5 of 59 cells did type *n* channels predominate. The majority of $CD4^-CD8^+$ cells exhibited *n*′ and *l* channels in various proportions, with *l* channels predominating in some and *n*′ channels predominating in others (Fig. 3C). These results are summarized in the tentative lineage diagram in Fig. 3D.

Our finding that immature thymocytes abundantly express type *n* K^+ channels agrees well with previous results from patch-clamp studies of thymocytes from humans (*18*) and mice (*19*). These reports demonstrate that *n* channels appear in the T lymphocyte lineage before the onset of immunological competence (Fig. 3D). Type *n*′ and *l* channels were not reported in an earlier study of $CD4^-CD8^+$ thymocytes (*19*), probably because the particular experimental protocols that distinguish among the several classes of K^+ channels were not used (see Fig. 1).

The preponderance of type *n* channels in double-negative, double-positive, and $CD4^+CD8^-$ cells and of type *n*′ and *l* channels in $CD4^-CD8^+$ cells raises the possibility that the channels have functions related to immunological activity or T cell development. Thus far, the functions of *n*′ and *l* channels in T lymphocytes are unknown. However, previous evidence suggests that expression of *n*-type K^+ channels in amounts of hundreds per cell is required for T cells to proliferate in response to mitogens (*1, 6, 20, 21*). These channels may play a similar role in thymocyte proliferation, because large double-positive and double-negative thymocytes, which account for the bulk of actively cycling cells in the thymus (*8*), have on average significantly greater numbers of *n* channels than do the largely quiescent $CD4^+CD8^-$ cells. An abundance of type *n* channels is not a sufficient mitogenic stimulus, however, as the channels are present at high density in postmitotic, small cortical thymocytes (small double-positive cells in Fig. 3A) and in resting human T cells (*1, 2, 21*). It has been suggested that small cortical thymocytes inherit their K^+ channels from the cortical blasts (*19*), by analogy to their "passive" acquisition of blast-cell TL antigen (*22*).

The expression of type *n*′ and *l* K^+ channels by $CD4^-CD8^+$ cells suggests that they may also be useful as cell-surface markers to identify possible precursors to the cytotoxic

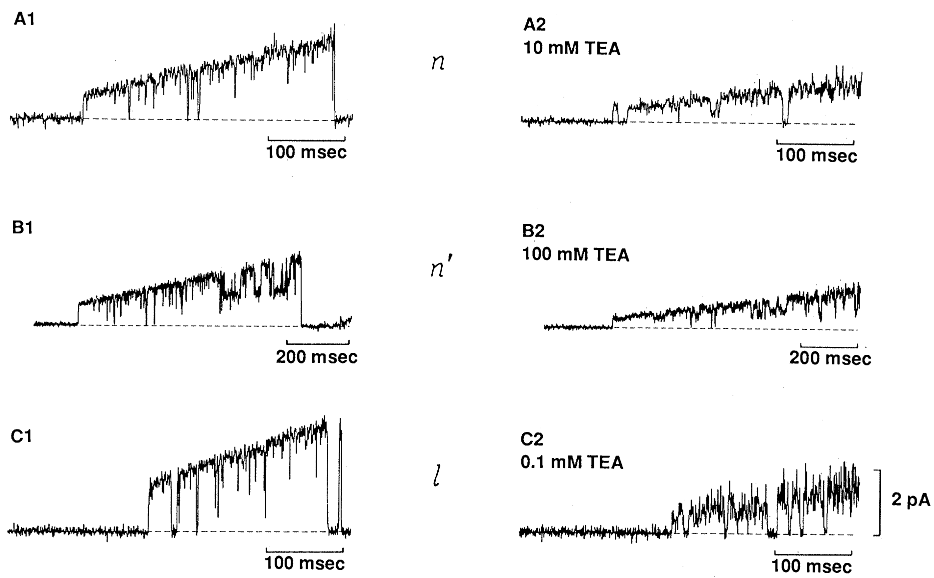

Fig. 2. Unitary conductances of three types of K^+ channels. (A) to (C) show multiple openings of single K^+ channels in three excised, outside-out patches, stimulated by voltage ramps from −60 to +80 mV in the absence or presence of bath-applied TEA. Pipette solution as in Fig. 1. Unitary conductance was determined from least-squares fits to the current through open channels. (**A**) An *n*-type K^+ channel with a slope conductance of 18 pS (A1); 10 m*M* TEA reduces the apparent single-channel conductance by 56% (A2). (**B**) An *n*′-type K^+ channel with conductance of 17 pS. A subconductance state of 10 pS is also evident (B1) ($CD4^-CD8^+$ cell); 100 m*M* TEA blocks the channel by 58% (B2). (**C**) An *l*-type K^+ channel with a conductance of 27 pS (C1) ($CD4^-CD8^+$ cell). The *l* channel is blocked 50% by 0.1 m*M* TEA (C2). The increased noise in the presence of TEA represents rapid blocking and unblocking events. Data were low-pass filtered at 800 Hz (A and C) or 400 Hz (B).

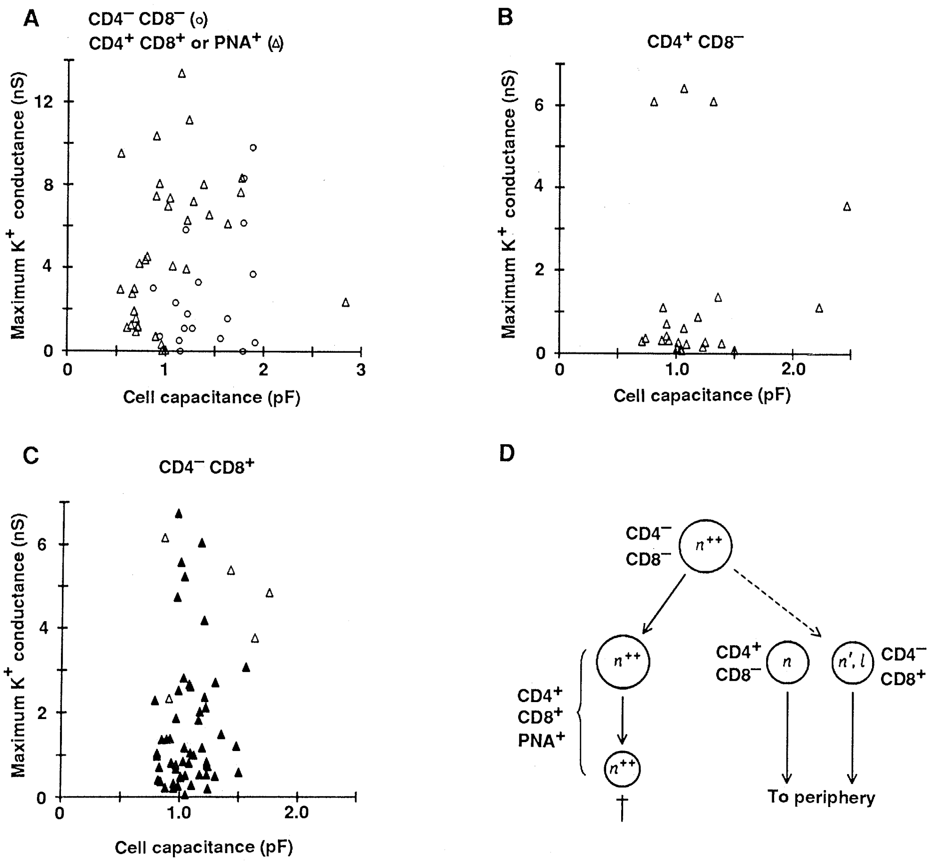

Fig. 3. Pattern of K^+-channel expression is linked to the cell-surface phenotype of thymocyte subsets. In (A) to (C), maximum K^+ conductance (g_K) is plotted against total membrane capacitance, a measure of membrane surface area (1 pF corresponds to $\sim 100\ \mu m^2$). For each cell, g_K was determined from a Boltzmann curve fitted to the K^+ conductance-voltage relation or from the current elicited at +30 mV, assuming a reversal potential of −80 mV. Capacitance was calculated from the average current transient evoked by a pulse from −80 to −70 mV, with correction for pipette capacitance. Open symbols represent cells with primarily type n channels, and closed symbols are those with type n' or l channels. (**A**) Double-negative and double-positive thymocytes. (**B**) $CD4^+CD8^-$ thymocytes. (**C**) $CD4^-CD8^+$ thymocytes. Cells in this class with large K^+ conductance ($g_K > 2$ nS) had either predominantly type n or l channels; the remainder generally expressed a combination of n' and l channels. (**D**) A simplified summary diagram relating K^+-channel expression to cell-surface phenotype and lineage in the thymus. The tentative lineage scheme is modified from (*8*). The dashed line reflects the uncertainty over the origins of mature T cells. Only the majority phenotype of $CD4^-CD8^+$ cells is indicated; a minority of $CD4^-CD8^+$ cells displayed large numbers of type n or l channels.

suppressor T cell lineage. Although much evidence suggests that mature T cells are ultimately derived from a double-negative thymic stem cell (*8–10, 23*), thymocytes may pass through an obligatory double-positive stage during maturation (*8, 9, 24*) (Fig. 3D). If precursor cells acquire n' or l channels prior to the mature $CD4^-CD8^+$ phenotype, then these channels should be detectable in a small fraction of double-negative or double-positive cells. In this regard it is interesting that type l K^+ channels are abundant in functionally defective $CD4^-CD8^-$ peripheral T cells from mice homozygous for the *lpr* gene mutation (*5, 6*). These cells are hypothesized to represent the aberrant expansion of a set of immature T cell precursors (*25*) and thus support the notion that a small population of normal immature thymocytes may express type l channels.

This report demonstrates that K^+-channel diversity is linked to the developmental fate of thymocyte subclasses. Cells destined to become MHC class II–restricted helper T cells ($CD4^+CD8^-$) have type n channels, whereas most of the cells that will become MHC class I–restricted cytotoxic or suppressor T cells ($CD4^-CD8^+$) express type n' and l K^+ channels. The stereotyped pattern of K^+-channel expression among subsets of normal thymocytes may offer important clues for future studies of the roles of K^+ channels in T cell development and function.

REFERENCES AND NOTES

1. T. E. DeCoursey, K. G. Chandy, S. Gupta, M. D. Cahalan, *Nature (London)* **307**, 465 (1984).
2. D. R. Matteson and C. Deutsch, *ibid.*, p. 468; M. D. Cahalan, K. G. Chandy, T. E. DeCoursey, S. Gupta, *J. Physiol. (London)* **358**, 197 (1985).
3. Y. Fukushima, S. Hagiwara, M. Henkart, *J. Physiol. (London)* **351**, 645 (1984).
4. P. Bregestovski, A. Redkozubov, A. Alexeev, *Nature (London)* **319**, 776 (1986).
5. T. E. DeCoursey, K. G. Chandy, S. Gupta, M. D. Cahalan, *J. Gen. Physiol.* **89**, 379 (1987).
6. K. G. Chandy *et al.*, *Science* **233**, 1197 (1986).
7. O. P. Hamill, A. Marty, E. Neher, B. Sakmann, F. J. Sigworth, *Pfluegers Arch.* **391**, 85 (1981).
8. R. Scollay, P. Bartlett, K. Shortman, *Immunol. Rev.* **82**, 79 (1984).
9. B. J. Mathieson and B. J. Fowlkes, *ibid.*, p. 141.
10. E. Rothenberg and J. P. Lugo, *Dev. Biol.* **112**, 1 (1985); B. Adkins *et al.*, *Annu. Rev. Immunol.* **5**, 325 (1987).
11. Thymocytes were isolated from BALB/c or C57BL/6 mice of either sex (4 to 8 weeks old) by gently pressing the thymus through a 500-mesh wire screen; the cells were washed and suspended in RPMI 1640 medium supplemented with 10% Hyclone fetal bovine serum and glutamine (suspension medium). Thymocytes prepared in this manner contain less than 0.5% macrophages or B cells [D. I. Beller and E. R. Unanue, *J. Immunol.* **121**, 1861 (1978); R. Scollay and K. Shortman, *Thymus* **5**, 245 (1983)]. Thymocytes (1×10^6 to 2×10^6) were stained with phycoerythrin (PE)-labeled antibody to CD4 (L3T4) at 5 μg/ml and fluorescein (FITC)-labeled antibody to CD8 (Lyt-2) at 25 μg/ml (monoclonal antibodies from Becton-Dickinson Immunocytometry Systems) in suspension medium for 20 to 30 minutes at 4°C. Cells were subsequently washed three times with suspension medium and stored at 4°C until use the same day. Prior to patch-clamp recording, stained cells were allowed to settle onto cover slip chambers treated with poly-D-lysine (Sigma) (0.25 mg/ml) and were visualized with a Zeiss IM 35 microscope equipped with a 100-W Hg lamp, fluorescein filter set, and ×63 Neofluar objective (oil; N.A. 1.25). To prevent photodynamic damage from biasing the results, excitation intensity was attenuated tenfold and the cells were illuminated for less than 5 seconds. In other experiments, individual unstained thymocytes were treated after patch-clamp recording with PNA-FITC (Vector Laboratories) (100 μg/ml) in the recording chamber and visualized.
12. S. B. Sands, R. S. Lewis, M. D. Cahalan, *Biophys. J.*, in press.
13. The blocking action of CTX is somewhat surprising in this case, considering previous evidence that the toxin is specific for Ca^{2+}-activated K^+ channels [C. Smith, M. Phillips, C. Miller, *J. Biol. Chem.* **261**, 14607 (1986)]. Activation of type n and n' K^+ channels does not appear to require intracellular Ca^{2+}, as both are opened by moderate depolarizations in the presence of less than 2 n*M* free Ca^{2+} (see Figs. 1 and 2). In fact, type n K^+ channels are inhibited by an increase in Ca_i^{2+} [P. Bregestovski, A. Redkozubov, A. Alexeev, *Nature (London)* **319**, 776 (1986); D. Choquet, P. Sarthou, D. Primi, P.-A. Cazenave, H. Korn, *Science* **235**, 1211 (1987)].
14. Type l channels are easily distinguishable from both n and n' channels; the selective blocking action of CTX allows the detection of single l channels in whole-cell recording even from cells expressing a great excess of n' channels. Similarities between n and n' channels would make positive identification of a small number of n' channels amid hundreds of n channels more difficult. In immature cells, a series of several repetitive depolarizations cause an almost complete cumulative inactivation of K^+ channels, indicative of type n channels (see Fig. 1A). In most cases the residual current elicited by the last pulse decays with a time course identical to that of the K^+ current elicited by the first pulse, indicating the lack of any measurable contributions from non-inactivating type n' channels.
15. D. P. Dialynas *et al.*, *J. Immunol.* **131**, 2445 (1983).
16. S. L. Swain, *Immunol. Rev.* **74**, 129 (1983).
17. P. Kisielow *et al.*, *Nature (London)* **253**, 219 (1975); H. Cantor and E. A. Boyse, *Cold Spring Harbor Symp. Quant. Biol.* **41**, 23 (1976).
18. L. Schlichter, N. Sidell, S. Hagiwara, *Proc. Natl. Acad. Sci. U.S.A.* **83**, 5625 (1986).
19. D. McKinnon and R. Ceredig, *J. Exp. Med.* **164**, 1846 (1986).
20. K. G. Chandy, T. E. DeCoursey, M. D. Cahalan, C.

McLaughlin, S. Gupta, *J. Exp. Med.* **160**, 369 (1984); T. E. DeCoursey, K. G. Chandy, S. Gupta, M. D. Cahalan, *J. Gen. Physiol.* **89**, 405 (1987).
21. C. Deutsch, D. Krause, S. C. Lee, *J. Physiol. (London)* **372**, 405 (1986).
22. E. Rothenberg, *J. Exp. Med.* **155**, 140 (1982).
23. R. Kingston, E. J. Jenkinson, J. J. T. Owen, *Nature (London)* **317**, 811 (1985).
24. L. Smith, *ibid.* **326**, 798 (1987).
25. R. C. Budd *et al.*, *J. Immunol.* **135**, 3704 (1985); H. C. Morse III *et al.*, *ibid.* **129**, 2612 (1982); D. Wofsy, R. R. Hardy, W. E. Seaman, *ibid.* **132**, 2686 (1984); A. N. Theofilopoulos *et al.*, *J. Exp. Med.* **153**, 1405 (1981).
26. S. Grissmer and M. D. Cahalan, in preparation.
27. We thank R. M. Davis for technical assistance, K. G. Chandy for stimulating discussions and comments on the manuscript, S. E. Fraser for advice on fluorescence microscopy, and C. Miller for a generous gift of charybdotoxin. This work was supported by NIH postdoctoral fellowship NS08021 (to R.S.L.) and by a research grant from the Arthritis Foundation and NIH grants NS14609 and AI21808 (to M.D.C.).

1 September 1987; accepted 31 December 1987

Expression of a Distinctive *BCR-ABL* Oncogene in Ph¹-Positive Acute Lymphocytic Leukemia (ALL)

STEVEN S. CLARK, JAMI MCLAUGHLIN, MICHAEL TIMMONS, ANN MARIE PENDERGAST, YINON BEN-NERIAH, LOIS W. DOW, WILLIAM CRIST, GIOVANNI ROVERA, STEPHEN D. SMITH, OWEN N. WITTE*

The Philadelphia chromosome (Ph¹) is a translocation between chromosomes 9 and 22 that is found in chronic myelogenous leukemia (CML) and a subset of acute lymphocytic leukemia patients (ALL). In CML, this results in the expression of a chimeric 8.5-kilobase *BCR-ABL* transcript that encodes the $P210^{BCR\text{-}ABL}$ tyrosine kinase. The Ph¹ chromosome in ALL expresses a distinct *ABL*-derived 7-kilobase messenger RNA that encodes the $P185^{ALL\text{-}ABL}$ protein. Since the expression of different oncogene products may play a role in the distinctive presentation of Ph¹-positive ALL versus CML, it is necessary to understand the molecular basis for the expression of $P185^{ALL\text{-}ABL}$. Both $P210^{BCR\text{-}ABL}$ and $P185^{ALL\text{-}ABL}$ are recognized by an antiserum directed to *BCR* determinants in the amino-terminal region of both proteins. Antisera to *BCR* determinants proximal to the *BCR-ABL* junction in CML immunoprecipitated $P210^{BCR\text{-}ABL}$ but not $P185^{ALL\text{-}ABL}$. Nucleotide sequence analysis of complementary DNA clones made from RNA from the Ph¹-positive ALL SUP-B15 cell line, and S1 nuclease protection analysis confirmed the presence of *BCR-ABL* chimeric transcripts in Ph¹-positive ALL cells. In Ph¹-positive ALL, *ABL* sequences were joined to *BCR* sequences approximately 1.5 kilobases 5′ of the CML junction. $P185^{ALL\text{-}ABL}$ represents the product of a *BCR-ABL* fusion gene in Ph¹-positive ALL that is distinct from the *BCR-ABL* fusion gene of CML.

THE LEUKEMIC CELLS OF MORE than 95% of CML patients (*1*) and of 5 to 20% of ALL patients (*2, 3*) carry the t(9;22)(q34;q11) translocation known as the Philadelphia chromosome (Ph¹) (*4*). In CML, the C-*ABL* gene on chromosome 9 is translocated into the middle of the *BCR* gene on chromosome 22 (*5*). Although the breakpoint on chromosome 22 is variable, it occurs within a defined 5.8-kb region of the *BCR* gene known as the breakpoint cluster region, or bcr (*6*). RNA splicing generates an 8.5-kb *BCR-ABL* chimeric transcript that is larger than the normal 6- and 7-kb C-*ABL* transcripts (*7, 8*). This results in the expression of the $P210^{BCR\text{-}ABL}$ protein (*9*) in which NH_2-terminal C-*ABL* sequences are replaced by sequences from the *BCR* gene (*10*).

Despite the fact that the Ph¹ chromosomes of CML and ALL are indistinguishable by cytogenetic analysis, cells from most Ph¹-positive ALL patients express *ABL*-derived protein and RNA species that are distinct from the *BCR-ABL* products of CML (*11, 12*). Ph¹-positive ALL cells display a high level of *ABL*-related tyrosine kinase activity in proteins of 180 and 185 kD, referred to collectively as $P185^{ALL\text{-}ABL}$ (*11*). Comparison of tryptic phosphopeptide maps between $P210^{BCR\text{-}ABL}$ and $P185^{ALL\text{-}ABL}$ revealed similar, but not identical, phosphorylation patterns suggesting some structural similarities (*11, 13*). The appearance of $P185^{ALL\text{-}ABL}$ correlates with the expression of a 6.5- to 7.0-kb *ABL* messenger RNA (mRNA) (*11–13*) in contrast to the 8.5-kb *BCR-ABL* transcript in CML cells. Genomic DNA analysis (*11–15*) and in situ hybridization studies (*15*) of the Ph¹ chromosome from ALL cells suggested that the breakpoint on chromosome 22 may not be in the bcr region as in the Ph¹ chromosome of CML. It is possible that a breakpoint elsewhere in the *BCR* gene, or within another gene on chromosome 22, could generate the altered *ABL* products in Ph¹-positive ALL. Alternatively, unusual RNA splicing within the *ABL* fusion partner may also account for the expression of $P185^{ALL\text{-}ABL}$.

To determine whether $P185^{ALL\text{-}ABL}$ contains *BCR* sequences, we compared the immunoreactivity of $P185^{ALL\text{-}ABL}$ and $P210^{BCR\text{-}ABL}$ with a panel of site-directed *BCR* antisera. Normal rabbit sera (NRS) did not recognize either protein (Fig. 1), while antisera directed against NH_2-terminal *BCR* sequences (antisera A) immunopre-

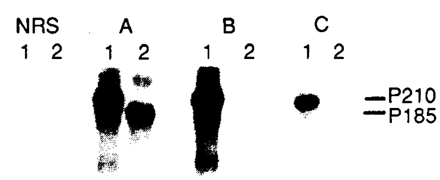

Fig. 1. $P185^{ALL\text{-}ABL}$ displays *BCR* homology limited to the NH_2-terminal region of *BCR*. K562 cells (*23*) (lanes 1) or the Ph¹-positive ALL cell line, ALL-1 (lanes 2) (*15, 24*) were immunoprecipitated with either normal rabbit serum (NRS) or with a panel of rabbit antisera raised against specific *BCR* determinants as illustrated in Fig. 2. Antiserum A was raised by immunizing rabbits with a *trpE-BCR* fusion protein expressed in the pATH-11 expression vector as described (*26*). Antigenic *BCR* sequences were encoded by a 1.4-kb Bam HI fragment (*8*). Antiserum B corresponds to the *BCR* 558 antiserum as reported (*10*). Rabbit antiserum C (*27*) was raised against a peptide sequence, IKSDIQREKRANKGSY, beginning 134 amino acids and 403 base pairs upstream of the *BCR-ABL* junction of K562 cells. The COOH-terminal tyrosine is not found in this position in the *BCR* sequence. Cell lysates were immunoprecipitated with the indicated antisera and prepared for the autokinase labeling reaction as described (*11*). The proteins were then reprecipitated with the same antisera used for the first cycle immunoprecipitation, separated by 8% SDS–polyacrylamide gel electrophoresis, and detected by autoradiography.

S. S. Clark, J. McLaughlin, M. Timmons, A. M. Pendergast, O. N. Witte, Department of Microbiology, Molecular Biology Institute and the Howard Hughes Medical Institute, UCLA, Los Angeles, CA 90024.
Y. Ben-Neriah, The Lautenberg Center for General and Tumor Immunology, The Hebrew University Hadassah Medical School, Jerusalem, Israel.
L. W. Dow and W. Crist, Department of Hematology/Oncology, St. Jude Children's Research Hospital, and Department of Pediatrics, University of Tennessee, Memphis, College of Medicine, Memphis, TN 38101.
G. Rovera, The Wistar Institute, Philadelphia, PA 19104.
S. D. Smith, Department of Pediatrics, Children's Hospital at Stanford, Palo Alto, CA 94304.

*To whom correspondence should be addressed.